Restoring Voluntary Bimanual Activities of Patients With Chronic Hemiparesis Through a Foot-Controlled Hand/Forearm Exoskeleton

Wenyuan Chen, Guangyong Li, *Member, IEEE*, Ning Li, Wenxue Wang, *Member, IEEE*, Peng Yu, Ruiqian Wang, Xiujuan Xue, Xingang Zhao, *Senior Member, IEEE*, and Lianqing Liu, *Senior Member, IEEE*

***Abstract*— A significant number of stroke patients are permanently left with a hemiparetic upper limb after the poststroke six-month golden recovery period, resulting in a drastic decline in their quality of life. This study develops a novel foot-controlled hand/forearm exoskeleton that enables patients with hemiparetic hands and forearms to restore their voluntary activities of daily living. Patients can accomplish dexterous hand/arm manipulation on their own with the assistance of a foot-controlled hand/forearm exoskeleton by utilizing foot movements on the unaffected side as command signals. The proposed foot-controlled exoskeleton was first tested on a stroke patient with a chronic hemiparetic upper limb. The testing results showed that the forearm exoskeleton can assist the patient in achieving approximately 107° of voluntary forearm rotation with a static control error less than 1.7°, whereas the hand exoskeleton can assist the patient in realizing at least six different voluntary hand gestures with a success rate of 100%. Further experiments involving more patients demonstrated that the foot-controlled hand/forearm exoskeleton can help patients in restoring some of the voluntary activities of daily living with their paretic upper limb, such as picking up food to eat and opening water bottles to drink, and etc. This research implies that the foot-controlled hand/forearm exoskeleton is a viable way to restore the upper limb activities of stroke patients with chronic hemiparesis.**

***Index Terms*— Wearable foot-machine interface, rehabilitation robot, hand exoskeleton, forearm exoskeleton.**

Manuscript received 30 August 2022; revised 2 December 2022; accepted 29 December 2022. Date of publication 2 January 2023; date of current version 2 February 2023. This work was supported in part by the National Natural Science Foundation of China under Grant 61925307, Grant U1908215, Grant 62003338, Grant 61933008, and Grant 61821005; and in part by the Liaoning Revitalization Talents Program under Grant XLYC2002014. *(Corresponding authors: Lianqing Liu; Guangyong Li.)*

This work involved human subjects or animals in its research. Approval of all ethical and experimental procedures and protocols was granted by the Rehabilitation Center for the Disabled of Liao Ning province, China.

Wenyuan Chen, Ning Li, and Ruiqian Wang are with the State Key Laboratory of Robotics, Shenyang Institute of Automation, Chinese Academy of Sciences (CAS), Shenyang 110016, China, also with the Institutes for Robotics and Intelligent Manufacturing, Chinese Academy of Sciences, Shenyang 110016, China, and also with the University of the Chinese Academy of Sciences, Beijing 100049, China (e-mail: chenwenyuan@sia.cn; lining3@sia.cn; wangruiqian@sia.cn).

Guangyong Li is with the Department of Electrical and Computer Engineering, Swanson School of Engineering, University of Pittsburgh, Pittsburgh, PA 15260 USA (e-mail: gul6@pitt.edu).

Wenxue Wang, Peng Yu, Xingang Zhao, and Lianqing Liu are with the State Key Laboratory of Robotics, Shenyang Institute of Automation, Chinese Academy of Sciences (CAS), Shenyang 110016, China (e-mail: wangwenxue@sia.cn; yupeng@sia.cn; zhaoxingang@sia.cn; lqliu@sia.cn).

Xiujuan Xue is with the Rehabilitation Center for the Disabled, Shenyang 110015, China (e-mail: xxj190003@163.com).

This article has supplementary downloadable material available at https://doi.org/10.1109/TNSRE.2022.3233631, provided by the authors.

Digital Object Identifier 10.1109/TNSRE.2022.3233631

I. Introduction

STROKE has become one of the leading causes of severe disability worldwide and has affected over 101 million survivors. Moreover, more than 12.2 million new stroke patients are diagnosed each year [1]. Hemiparesis of the upper limb is a common complication following stroke, and it diminishes the quality of life of stroke survivors drastically. Considering that the hand/forearm is responsible for nearly 90% of upper limb functions [2], [3], hand/forearm function assistance has gained increasing attention in the field of assistive device research. Recently, several hand [4], [5] and forearm exoskeletons [6], [7], [8] have been developed for rehabilitation after stroke, but few have been designed to assist patients in their daily activities. In fact, a significant number of stroke patients are permanently left with a hemiparetic hand and forearm after the poststroke six-month golden recovery period [9]. Therefore, there is a much higher demand for hand/forearm exoskeletons for activities of daily living (ADLs) than for rehabilitation.

Control of hand exoskeletons for ADLs requires the detection of a patient's intention to move, which is considered to be very challenging. Currently, a variety of signals have been tried for controlling hand exoskeletons, for instance: (1) button-triggering [10], [11]; (2) physiological signals such as electroencephalogram (EEG) and electromyography (EMG) [12], [13], [14], [15]; (3) voice [16] or computer vision [17]; and (4) body movements such as ipsilateral thumb movements [18], contralateral shoulder movements [19], and eye movements [20]. Among these signals, EEG and EMG have shown great potentials. However, they are still not reliable enough now to detect the desired motion intentions. For example, EEG has very low signal-to-noise ratio, often resulting in unreliable control of the hand exoskeleton. EMG has demonstrated some success, such as Myomo in [15], however, it is only suitable for very few stroke patients with sufficient EMG signal strength in their forearm muscles, while most patients unfortunately have very low-level and unstable muscle activation because of the stroke. Other signals are too simple to generate a complex motion intention for stroke patients to restore their voluntary ADLs through the hand exoskeleton.

To solve this problem, we propose a hand exoskeleton that allows stroke patients to generate various gestures of their hemiparetic hand using a foot-machine interface (FMI). The FMI is inspired by the fact that the anatomy and kinematics of the human foot are similar to those of the hand. Therefore, the FMI is more intuitive than other body interfaces. A button to activate and deactivate the foot control mode is integrated with the FMI to prevent walking activity from interfering with hand activities.

Currently, FMIs have been designed to teleoperate a robotic system when the user's hands are busy. Several FMIs [21], [22], [23], [24] command a slave robot using switches placed on a planar base. These interfaces are simple to use but cannot perform movements with more than three degrees of freedom (DOFs) [25]. Additionally, continuously lifting a leg up and down during teleoperation may cause user fatigue [26]. Therefore, Huang et al. proposed a pedal with eight feedback-sensing modules to control the four DOFs of a slave robotic arm by collecting foot gestures [25]. However, the pedal restricts the mobility of the operator, and it is inconvenient to use it in controlling the hand exoskeleton. Recently, some fully wearable FMIs have been reported for prostheses to recognize the motion intention of amputees, which may also be suitable for controlling hand exoskeletons. Lyons et al. designed an upper limb prosthesis controlled via the surface EMG of leg gestures [27]. However, biomechanical coupling between leg movements often causes the misclassification of some gestures. A wearable FMI was reported in [28] utilizing two Inertial Measurement Units (IMUs) located on the feet to control prosthetic upper limbs. Each foot is capable of operating up to 8 hand/arm movements. However, a tedious process of "re-zero" is needed every time the body is repositioned (e.g. standing to reclined sitting). A wearable FMI using pressure sensors placed on the big toes to detect the motion intention of the user was reported in [29] to control the abduction and flexion motions of an artificial thumb. Another wearable FMI using four pressure switches on the insole, similar to the button-triggered control method, was reported in [30] to activate four pre-programmed hand movements of the prosthesis. The aforementioned FMIs can only generate a few commands because each sensor corresponds to only one gesture. Therefore, it is impossible to use them to control dexterous movements of hand exoskeletons.

In this study, we designed an FMI using piezoresistive sensors placed on the sole and toes, which can perceive multiple intentions of the patient using a combination of sensor outputs, to voluntarily control various hand gestures of the exoskeleton. The configuration of the plantar sensors was optimized based on an analysis of the anatomy and kinematics of the human ankle-foot system. Four piezoresistive sensors are used to generate up to 16 different commands. In this study, only six foot gestures are chosen to control six common hand gestures for ease of operation.

Our previous study demonstrated that a hand exoskeleton with actuated thumb and finger movements can assist patients with chronic hemiparesis in accomplishing some of the coarse grasping tasks without involving forearm [31]. However, forearm pronation/supination (P/S) motions play a major role in voluntary ADLs, such as bringing food to the mouth and preventing the water in the cup from spilling [32]. It is impossible for most post-stroke survivors, who usually also have a paretic forearm, to constantly rotate the forearm to adjust the orientation of the grasped object when executing ADLs. Therefore, this study will combine hand gesture assistance with forearm rotation assistance to achieve voluntary ADLs for patients with chronic hemiparetic upper limbs. Most forearm exoskeletons available for assisting pronation and supination cannot be used as daily assistance devices because they are typically fixed on a platform [6], [7], [8]. Several wearable forearm exoskeletons can rotate the forearm using an arc-shaped rail [33], [34] to guide a rotator attached to the forearm. However, the arc-shaped rail is bulky, and it is difficult to don these forearm exoskeletons along with hand exoskeletons. Soft helical actuators have also been designed for forearm P/S motions [35], [36]. However, they are limited by a small actuation torque, and their effectiveness has not yet been validated in patients. To the best of our knowledge, there is currently no device capable of providing simultaneous active hand gestures and forearm rotation assistance for ADLs in patients with hemiparesis.

This study develops a forearm exoskeleton for P/S assistance that can be integrated with a hand exoskeleton. For most ADLs, hand movements and forearm P/S are sequentially executed. During hand movements, multiple hand gestures are performed to grasp and hold objects of different shapes and sizes. Moreover, the forearm is continuously rotated to ensure the grasped object is rotated with an appropriate orientation during forearm P/S movements. Therefore, in contrast to the aforementioned FMI for hand gesture control, forearm P/S movements are continuously controlled by pressing two piezoresistive sensors. Besides, an additional foot gesture is predefined to switch between forearm and hand control modes. The performance of the foot-controlled forearm exoskeleton is evaluated experimentally in two patients with chronic hemiparesis. Both patients could voluntarily complete several ADLs, such as unscrewing the bottle cap, drinking, and eating, with the assistance of the foot-controlled hand/forearm exoskeleton system.

The main contribution of this article is summarized as follows. On the one hand, the proposed exoskeleton can simultaneously provide both active hand and forearm rotation assistance; on the other hand, by utilizing healthy foot movements as command signals, patients can accomplish dexterous hand/arm manipulation on their own with the assistance of a foot-controlled hand/forearm exoskeleton. Therefore, stroke patients are able to voluntarily accomplish bimanual ADLs such as unscrewing the bottle cap, drinking, and eating. To the best of our knowledge, this is the first wearable hand/forearm exoskeleton can restore voluntary bimanual activities of stroke patients.

The remainder of this paper is organized as follows. Section II introduces the system design of the foot-controlled hand/forearm exoskeleton, which is further elaborated in Section III. Section IV provides the experimental methods, results, and discussion. Finally, the conclusion is presented in Sections V.

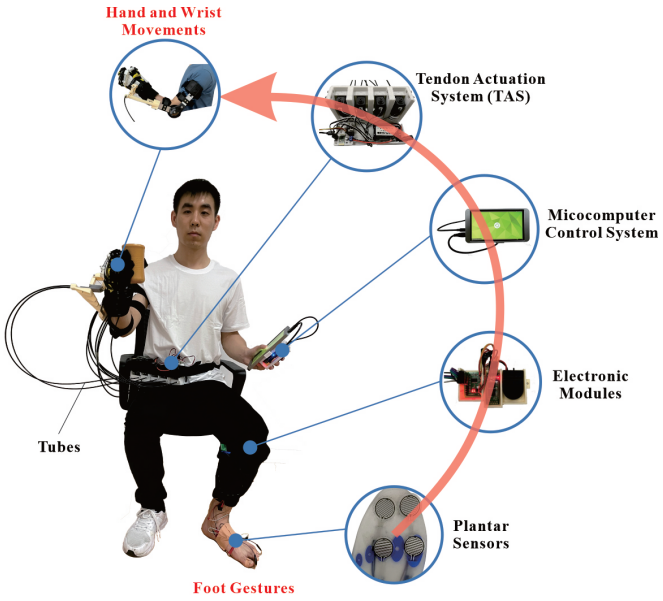

Fig. 1. Foot-controlled hand/forearm exoskeleton is composed of four subsystems: a wearable hand/forearm exoskeleton, a tendon actuation system (TAS), a wearable FMI, and a microcomputer computer control system. The subject gave his permission for this photograph to be reproduced.

Fig. 2. Tendon actuation schematic of the hand exoskeleton.(a) Palmar and (b) dorsal views.

II. System Design

As shown in Fig. 1, the entire system is composed of four main modules: (1) a wearable hand/forearm exoskeleton that performs digits movements and forearm rotation; (2) a remote tendon actuation system (TAS) that drives the hand/forearm exoskeleton; (3) a wearable FMI that recognizes foot gestures through plantar sensors; and (4) a microcomputer control system that takes the sensor reading, deciphers foot gestures, maps foot gestures to hand gestures and mode switch, directly controls the TAS.

A. Hand Exoskeleton

Tendon-actuated hand exoskeletons have attracted widespread interest of researchers because of their light weight and compact size [10], [11]. Tendons are usually designed to replicate hand muscles, making the movements generated by the hand exoskeleton much more similar to natural hand movements [37]. However, some complicated movements, such as thumb movements, are actuated by many muscles that are difficult to generate through replications. Therefore, tendon-actuated hand exoskeletons reported in the literature do not consider much active thumb actuation, and most can only assist the patient in performing simple gestures, such as grasping and releasing. To solve this problem, we designed a tendon-actuated hand exoskeleton with fully actuated thumb movements for grasping assistance, as described in our previous study [31]. As shown in Fig. 2, the routing of tendons in the hand exoskeleton is summarized as follows. A hybrid actuation mechanism that combines two tendons (thumb abductor and adductor) and a flexible link performed thumb abduction and adduction movements. The flexor and extensor tendons of each finger were used to generate flexion and extension movements. These biomimetic tendons are controlled by four actuators to perform the following hand motions: thumb abduction and adduction, thumb flexion and extension, index flexion and extension, and simultaneous flexion and extension of other three fingers. Consequently, for dexterous operations, the entire hand exoskeleton system can achieve 4-DOF movements.

Our previous study [31] confirmed that four DOFs were sufficient for stroke patients to accomplish training tasks and some ADLs. However, the hand exoskeleton was controlled by a touch screen, causing occupancy of the patient's hand on the unaffected side, making it impossible for the patient to complete voluntary bimanual manipulations. The wearable FMI proposed in this study allows patients to control the hand exoskeleton using their foot on the unaffected side. Therefore, dexterous operations can be achieved through the collaboration of both hands. The design of the wearable FMI, inspired by the analysis of the anatomy and kinematics of the human foot, is discussed in Section II-C.

B. Forearm Exoskeleton

In addition to hand assistance, forearm P/S assistance is indispensable during the execution of ADLs because the paretic forearm of patients is usually too weak to rotate on their own. So far, according to the best of our knowledge, there are no exoskeletons reported in literature that can simultaneously provide both hand and forearm P/S assistance. In this study, we proposed a tendon-actuated forearm exoskeleton for forearm P/S assistance that can be easily integrated with the hand exoskeleton reported in our previous study [31]. The forearm exoskeleton consists of an arm-fixed brace, a sliding mechanism, and a parallelogram mechanism, as shown in Fig. 3. The brace is attached to the arm of the patient, and its length can be adjusted using a sliding mechanism. A parallelogram mechanism was used to rotate the forearm of the patients,

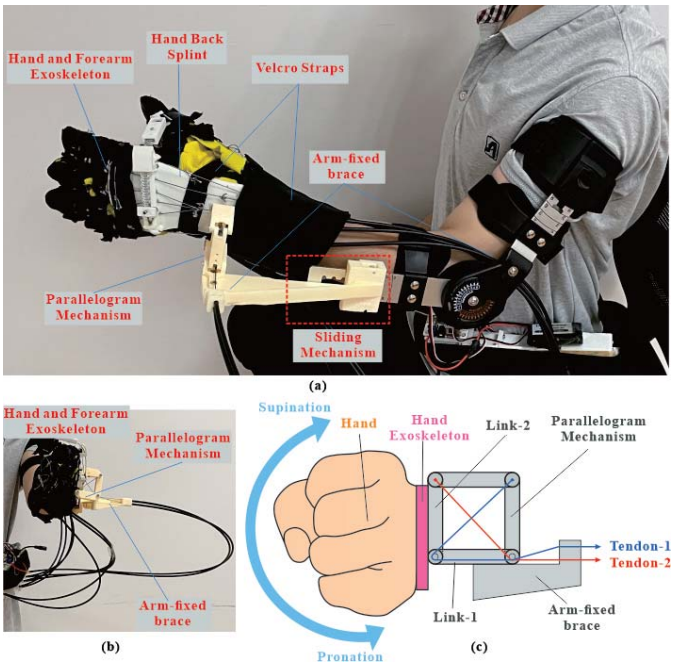

Fig. 3. Tendon-driven forearm exoskeleton for the assistance of pronation/supination movements. (a) Side view and (b) Front view of the forearm exoskeleton worn by the participant. (c) Schematic of the tendon-driven mechanism of the forearm exoskeleton.

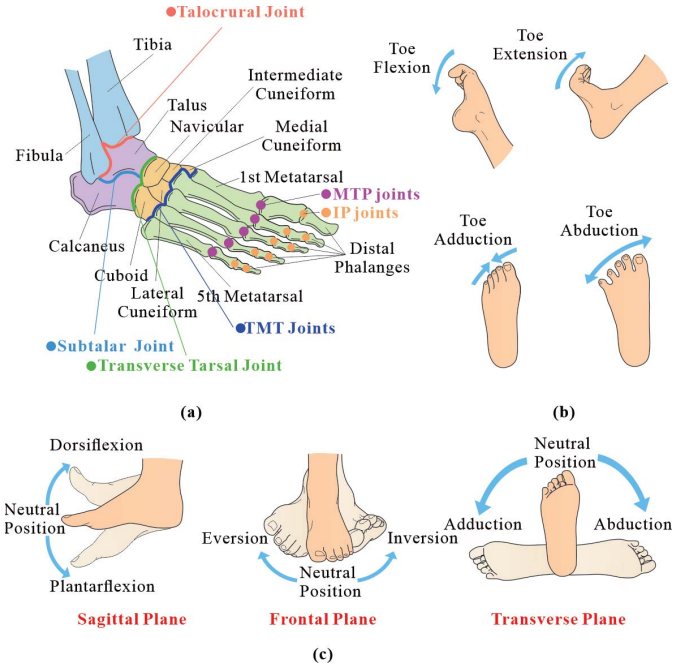

Fig. 4. Anatomy and kinematics of the ankle-foot system. (a) Anatomical bones and joints of the ankle-foot system. Movement of the (b) foot and (c) ankle.

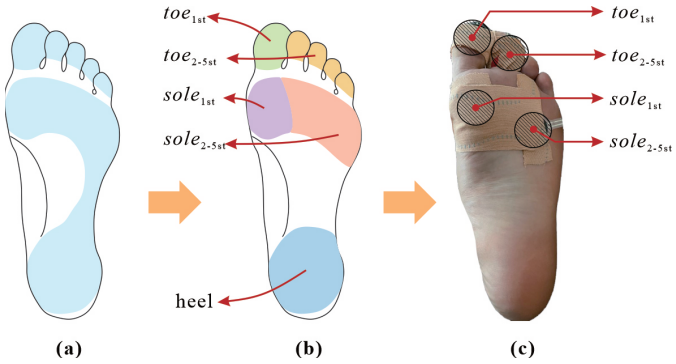

Fig. 5. Design schematic of the FMI. (a) Plantar sensitive area during normal walking. (b) Five areas divided based on the kinematics of the ankle and foot. (c) Four piezoresistive sensors placed on the forefoot areas. The heel area is abandoned because it is the farthest from other areas and difficult to be treaded together with other areas.

as shown in Fig. 3(c). Link-1 and Link-2 of the parallelogram mechanism were fixed to the arm-fixed brace and hand exoskeleton, respectively. Consequently, the rotation of the parallelogram mechanism actuated by the tendons causes the forearm to rotate. Specifically, the forearm supinates when Tendon-2 was pulled and Tendon-1 was released. Conversely, the forearm pronates when Tendon-1 was pulled and Tendon-2 was released.

The paretic wrists of stroke patients maintain an excessive amount of flexion, making it impossible to adjust their hands to an appropriate posture for grasping objects and performing ADLs. Nevertheless, wrist flexion and extension are not necessary during ADLs, which require the wrist to be maintained in a suitable posture. Therefore, the forearm exoskeleton in this study provides a passive wrist support to aid patients in maintaining their wrists in a neutral posture, which is sufficient for performing most ADLs. The hand back splint used to support the wrist of patients is fastened around their wrist using two Velcro straps. Passive wrist support does not affect the forearm P/S and hand assistance of patients but make grasping and operation easier while carrying out ADLs. Furthermore, passive wrist support does not increase the weight of the entire exoskeleton system because no additional actuators are required.

C. Wearable FMI Design

In this study, the anatomy and kinematics of the foot were first analyzed to optimize the configuration of the plantar sensors and maximize the number of commands generated through the foot movements, which is introduced in a supplementary PDF. Some key anatomical and kinematic features of the ankle-foot system that can be utilized for the design of the FMI are summarized as follows: As shown in Fig. 4, (1) the ankle joints can generate 2-DOF movements with a wide range: dorsiflexion/plantarflexion and eversion/inversion; (2) all the toes can accomplish large range flexion and extension movements; and (3) the hallux is independent of the other toes.

The sensitive plantar tactile sense is formed by dense cutaneous receptors on the soles of the foot, controlling human stance and locomotion. With tactile feedback, the user can precisely tread the areas on the soles while performing foot movements. For this reason, we designed an FMI to detect the foot movements of users through plantar piezoresistive sensors. The number and location of plantar sensors were optimized based on the aforementioned analysis of ankle-foot anatomy and kinematics.

The sensitive plantar area during normal walking is shown in Fig. 5(a), which is divided into forefoot and heel areas, as shown in Fig. 5(b). Based on the kinematics of the ankle

and foot, the forefoot areas are further divided into four areas that can be treaded by repeatable ankle and foot movements as follows: the first sole ($sole_{1st}$), second to fifth soles ($sole_{2-5st}$), first toe (toe_{1st}), and second to fifth toes (toe_{2-5st}). A piezoresistive sensor was placed in each area of the forefoot, as shown in Fig. 5(c), which can be treaded individually or in combination to generate control commands. The heel area was abandoned in this study because it was the farthest from other areas and difficult to be treaded together with other areas. Consequently, the maximum number of generated actions N using four plantar sensors is 16 according to the following equation, which meets the control requirements of the dexterous hand exoskeleton.

$$N = \sum_{k=0}^{4} C_4^k = 16 \tag{1}$$

where C_n^k is the binomial coefficient of n and k, defined as follows:

$$C_n^k = \frac{n!}{(n-k)! \cdot k!} \tag{2}$$

The electronic modules of the FMI are worn on the leg of the user and consist of a signal acquisition module, Bluetooth transmission module, and Li-Po battery. The signal acquisition module amplifies and discretizes the four sensor values and sends them to the microcomputer control system using Bluetooth. The microcomputer control system analyzes the plantar sensor values and generates commands for the hand/forearm exoskeleton. As described in Section I, the wearable FMI is designed with the following two switchable control modes: 1) hand control mode and 2) forearm control mode, which can be switched back and forth using a predefined foot gesture.

1) Hand control mode: The target hand gestures (M0 to M5) that are commonly used in ADLs, including four DOFs and their combined gestures of the hand exoskeleton are shown in Fig. 6. For ease of statement, we defined thumb abduction, thumb flexion, index flexion, and other finger flexions as four activated DOFs. Additionally, thumb adduction, thumb extension, index extension, and other finger extension are defined as four unactivated DOFs. As a result, M0 is the gesture with four unactivated DOFs, encoded as [0 0 0 0]; M1 is the gesture with a single activated DOF of thumb abduction, encoded as [1 0 0 0]; and M2 to M5 are the combined gestures with multiple activated DOFs.

To control the hand exoskeleton conveniently, we predefined six foot gestures (G0 to G5), as shown in Fig. 6. The mapping from foot to hand gestures is shown in Table I. Specifically, we defined three states of the ankle joint in the sagittal plane (01 denotes dorsiflexion (DF), 00 denotes neutral position (NP); and 10 denotes plantarflexion (PF)), three states of the ankle joint in the frontal plane (01 denotes eversion (EV), 00 denotes neutral position (NP), and 10 denotes inversion (IN)), two states of the hallux joints (0 denotes extension(E), and 1 denotes flexion (F)), and two states of the other toe joints (0 denotes extension(E) and 1 denotes flexion (F)). The foot gesture G0, encoded as [01, −, −, −], maps to the M0 hand gesture. In this case, none of the sensors are pressed. The foot gesture G1, which exerts pressure primarily on one sensor

Fig. 6. Hand gestures of the hand exoskeleton corresponding to the foot gestures. The activated DOFs of the hand gestures are encoded as marked in the images below.

TABLE I
MAPPING FROM FOOT GESTURES TO HAND GESTURES

Hand Movements	Ankle Joint (Sagittal Plane)	Ankle Joint (Frontal Plane)	Hallux Joints DOFs	Toe Joints DOFs
M0	0 1	–	–	–
M1	0 0	1 0	0	0
M2	1 0	0 0	1	1
M3	0 0	1 0	1	1
M4	0 0	0 1	1	1
M5	0 0	0 0	1	1
Switch	0 0	0 1	0	0

($sole_{1st}$), is encoded as [00, 10, 0, 0] and maps to the hand gesture with a single activated DOF (M1). By analogy, foot gestures G2 to G5 exert strong pressure on multiple sensors, thereby mapping the hand gestures with multiple activated DOFs.

2) Forearm control mode and control mode switch: As patients need to constantly adjust the postures of the forearm while carrying out ADLs, the rotation angle of the forearm is continuously controlled using FMI. Therefore, a switch mechanism is required to toggle between hand and forearm control modes. An additional foot gesture, G_{switch}, encoded as [00 01 0 0], can serve as a switching signal. The switch is convenient to handle and not easily confused with other foot gestures because only one sensor ($sole_{2-5st}$) exerts pressure, as shown in Fig. 6 and Table I. In the forearm control mode, the supination and pronation of the forearm are controlled by two pressure sensors. Specifically, the forearm supinates at a uniform speed when pressing $sole_{1st}$ and pronates at a uniform speed when pressing toe_{1st}. Switching back to the hand control mode can be realized by utilizing the G_{switch} again.

D. Tendon Actuation System and Microcomputer Control System

The tendon actuation system (TAS) tied around the waist, as shown in Fig. 1, consists of five micro servo motors (LDX-227, Hiwonder, China), five bidirectional pulleys,

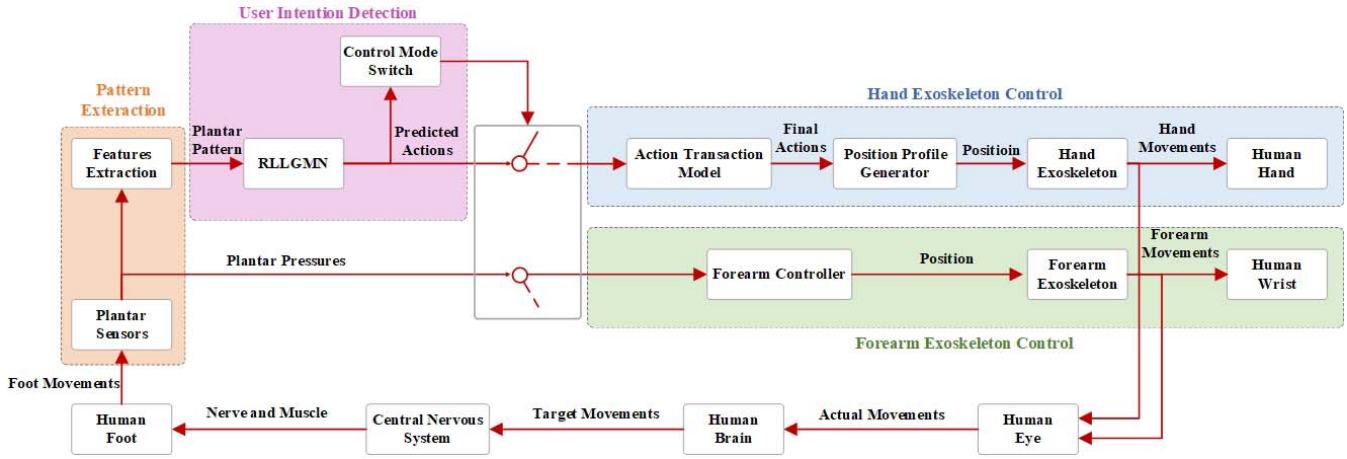

Fig. 7. Control diagram of the foot-controlled hand/forearm exoskeleton, which can be summarized into four main modules besides the user: pattern extaction, user intention detection, hand exoskeleton control, and forearm exoskeleton control.

a custom-made driver board (LSC-6, Hiwonder, China), and a Li-battery. Each motor can output a maximum torque of 15 kg·cm and rotation angles of 0–270°, connecting the biomimetic tendons through one bidirectional pulley. The bidirectional pulley can pull one tendon and simultaneously release another, and vice versa, thus reducing the number of motors needed. Consequently, dexterous hand and forearm movements of the exoskeleton can be controlled through only five motors.

Fig. 1 shows the microcomputer control system, which provides a graphic user interface (GUI) for patients to select two kinds of control modes: direct control by touching the screen and foot-controlled mode. In the foot-controlled mode, a single-board computer (Raspberry Pi 4B) connected to the FMI via Bluetooth was used to take the sensor reading, decipher foot gestures, map foot gestures to hand gestures and mode switch, directly control the TAS. The control algorithms are described in detail in Section III.

III. System Control

Figure 7 shows the control diagram of the foot-controlled hand/forearm exoskeleton, which can be summarized into four main modules: pattern extraction, user intention detection, hand exoskeleton control, and forearm exoskeleton control.

1) Pattern Exaction: The plantar pressure from four piezoresistive sensors are measured and then converted to discrete signals $F_j(k)$, where $j = 1, 2, 3, 4$, correspond to the label of each sensor. These signals are further normalized to $x_j(k)(j = 1, 2, 3, 4)$ using the following formula:

$$x_j(k) = \frac{F_j(k) - F_j^{\min}}{F_j^{max} - F_j^{min}} \tag{3}$$

where F_j^{min} is defined as the minimum value of $F_j(k)$, which is measured while the sensor with label j is relaxed, and F_j^{max} is defined as the maximum value of $F_j(k)$, which is measured while the sensor with label j is pressed.

The time-series features of every pressure signal sequence are extracted using a time window with a fixed length N, which is expressed as

$$\boldsymbol{X}_j(k) = \left[x_j(k), x_j(k-1), \ldots, x_j(k-N+1)\right] \tag{4}$$

Subsequently, we define the plantar pattern matrix at the current time $\boldsymbol{X}(k)$ as follows:

$$\boldsymbol{X}(k) = [\boldsymbol{X}_1(k), \boldsymbol{X}_2(k), \boldsymbol{X}_3(k), \boldsymbol{X}_4(k)]^T \tag{5}$$

which is the input of the user intention detection module.

2) User Intention Detection: The recurrent log-linearized Gaussian mixture network (R-LLGMN) proposed in [38] can perform temporal pattern classification. Hence, it was used in this study to detect the user intention from the plantar pattern matrix. The R-LLGMN predicts the current user action $a(k)$ from the following probability vector $\boldsymbol{u}(k)$.

$$\begin{aligned}\boldsymbol{u}(k) &= [u_1(k), u_2(k), \ldots, u_i(k), \ldots, u_Q(k)] \\ &= F^{\text{trans}}(\boldsymbol{X}(k))\end{aligned} \tag{6}$$

where $u_i(k)(i = 1, 2, \ldots, Q)$ is defined as the probability of the ith action that the user intends to execute; Q is the total number of actions; and $F^{trans}(\cdot)$ is the function of the R-LLGMN. The following condition is satisfied:

$$\sum_{i=1}^{Q} u_i(k) = 1 \tag{7}$$

Finally, the current action, $a(k)$ was chosen from those with a higher probability by considering the history of actions to minimize the prediction error. In this study, we used a finite-state machine to describe the transition of these actions, as shown in Fig. 8, and the start action, $a(0)$ is set as the opening state (M0). Consequently, the current action was determined according to the path indicated by arrows in Fig. 8 if the corresponding transition event occurs; otherwise, the current action, $a(k)$ is determined as the previous action $a(k-1)$. In addition, transition events, T_i are defined as follows:

$$T_i : u_i(k) > \varepsilon_i, i = 1, 2, \ldots, Q \tag{8}$$

where ε_i is defined as the threshold of the ith action, which is experimentally configured in advance.

3) Hand Exoskeleton Control: After the action, $a(k)$ is determined, the hand exoskeleton performs the corresponding movements. Specifically, a position profile generator constructs the commanded motor profiles, $p_{cmd}(t)$ based on the

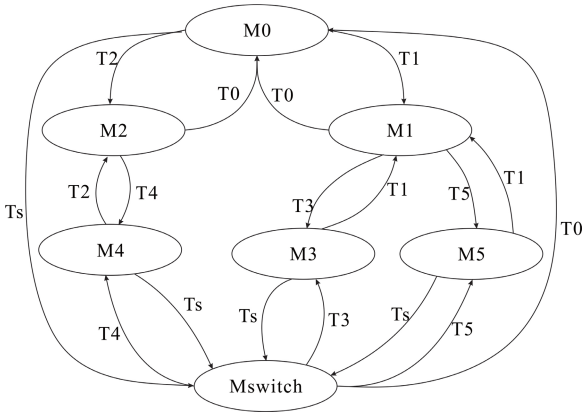

Fig. 8. Action transaction model. M0 to M5 denote the hand movements; M_{switch} denotes the action of the control mode switch; and T_i denotes transition events.

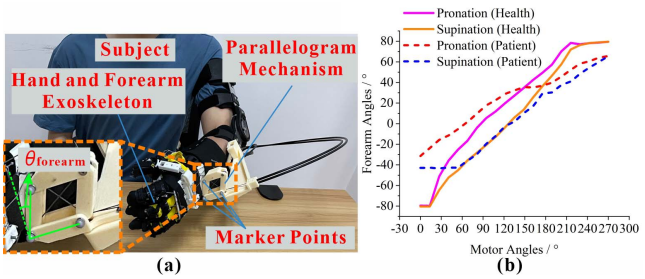

Fig. 9. Mechanical evaluation of the forearm exoskeleton. (a) The forearm rotational angles are measured by optical capture system. (b) Relationship between the forearm and servomotor rotational angles during supination and pronation assistance.

minimum-jerk principle, which can maximize the smoothness of the profiles [39], [40]. The commanded motor profiles are expressed as follows:

$$p_{cmd}(t) = p_0 + (p_T - p_0) \cdot \left(10\left(\frac{t}{T}\right)^3 - 15\left(\frac{t}{T}\right)^4 + 6\left(\frac{t}{T}\right)^5\right) \quad (9)$$

where p_0 and p_T are the position of the motors at the inital time 0 and end time T of the action period, respectively.

Within the action period, the position controller applies proportional and derivative control, as follows:

$$v_{cmd} = k_p \cdot (p_{cmd} - p) - k_d \cdot v \quad (10)$$

where k_p and k_d are the proportional gain and derivative gain; p_{cmd} and p are commanded and measured motor positions, respectively; and v_{cmd} and v are commanded and measured motor velocities, respectively.

4) Forearm Exoskeleton Control: The rotation movements of the forearm are directly controlled by the discrete signals of sensors, $sole_{1st}$ and toe_{1st} (i.e., $F_1(k)$ and $F_2(k)$). The forearm controller shown in Fig. 7 is designed according to the following control law, which is given by

$$\theta_k = \begin{cases} \theta_{k-1} + \Delta\theta, & \text{if } F_1(k) > \epsilon \\ \theta_{k-1} - \Delta\theta, & \text{if } F_2(k) > \epsilon \end{cases} \quad (11)$$

where θ is the rotational angle of the forearm actuator; ϵ is the activation threshold of the forearm rotation; and $\Delta\theta$ is the velocity of θ change, which can be set in advance by users according to their comfort level.

Within the action period, the forearm actuator is controlled based on proportional and derivative controls, similar to the hand actuator, as shown in Eq. (10).

IV. Results and Discussions

In this section, we experimentally evaluate the feasibility of the foot-controlled hand/forearm exoskeleton for restoring voluntary activities of patients with chronic hemiparesis. Two patients with a hemiparetic arm and a healthy participant participated in the experiments. The details of the participants are summarized in Table S1. All experiments were approved by the Rehabilitation Center for the Disabled of Liao Ning province, China, and conducted as follows.

A. Mechanical Evaluation of Forearm Exoskeleton

In the first experiment, the mechanical parameters (i.e., rotational angle) of the forearm exoskeleton were measured on both participants to evaluate its performance on forearm P/S assistance. The mechanical evaluation of the hand exoskeleton was not included in this study, as it has been described in our previous study [31].

During the measurement, two participants (the healthy participant and stroke patient 1) kept their arms dangling, and the forearm was pronated and supinated under the actuation of the forearm exoskeleton, as shown in Fig. 9(a). The rotational angles of the forearm and servomotor were measured using an optical capture system (OptiTrack, LEYARO, China) and a potentiometer, respectively. As a result, we obtained the relationship between the rotational angles of the forearm and servomotor, as shown in Fig. 9(b). The measurement results indicate that the forearm exoskeleton can assist the healthy participant in generating approximately 80° pronation and 80° supination motions. The range of forearm rotation motion is approximately 160°, which meets the requirement for ADLs according to [41]. The forearm exoskeleton can assist the patient in generating approximately 42° pronation and 65° supination motions. The range of forearm rotation motion of the patient is approximately 107°, which is approximately 67% of that of the healthy participant, making it possible for the patient to perform some ADLs voluntarily, as demonstrated in the Supplementary video.

B. Evaluation of the FMI

The performance of the FMI was evaluated to validate its effectiveness in voluntarily controlling the exoskeleton by the patient 1 under two separate control modes: hand control and forearm control. Before the actual experiments, a short training session was provided for the patient. First, we demonstrated all foot gestures to the patient and explained the mapping from foot gestures to hand gestures, as introduced in Section II-C. Then, we allowed the patient to practice a few times and become familiar with every foot gesture.

While conducting the hand control experiment, the patient was asked to continuously perform some foot gestures by following the target hand gestures displayed on a screen.

During this period, the plantar pattern matrix, X(k) and target hand gestures were recorded and stored in the memory, which was extracted in batches to train the R-LLGMN using the stochastic gradient descent (SGD) optimizer. In this experiment, k is set to 10, therefore, the size of X(k) is 10×4. The training data collection takes about 120 seconds, and the collected sample data size was $300 \times 10 \times 4$. The number of training iterations was set to 1000. The RLLGMN training takes about 30 seconds. The trained R-LLGMN was then employed to control the hand exoskeleton using the aforementioned control method. Subsequently, the patient was asked to operate the hand exoskeleton using the foot on the unaffected side to follow some random targeted hand gestures or the mode switch command displayed on the screen. Note that, for ease of hand control evaluation, the mode switch was closed, and the exoskeleton control mode remained unchanged during the hand control experiment. In addition, a brief pause occurs when switching these targeted gestures to allow the patient to switch foot gestures. The results of the hand control experiment, as shown in Fig. 10(a), demonstrate that the patient can easily switch hand gestures and perform every hand gesture with a success rate of 100%.

While conducting the forearm control experiment, the patient was asked to operate the foot-controlled forearm exoskeleton to first reach a static target and then track a dynamic trace of the forearm P/S movements displayed on the screen. Moreover, the forearm rotational angle, θ is displayed on the screen to provide feedback to the patient. θ is calculated using the motor rotational angle based on the relationship between the motor and forearm rotational angles, as described in Fig. 9(a). Each experiment was conducted ten times for every static target forearm angle, and the errors between the reached angles and targeted angles were recorded. The patient could rotate his forearm to specific targeted angle with static error less than 1.7°, as shown in Fig. 10(b).

The results of these two experiments indicate that the proposed FMI is capable of voluntarily controlling the hand/forearm exoskeleton with satisfactory accuracy.

C. Performance of Foot-Controlled Hand/Forearm Exoskeleton in Activities of Daily Living

In this experiment, two patients were asked to accomplish the following unimanual (a-c) and bimanual (d-g) tasks with the assistance of a foot-controlled hand/forearm exoskeleton:

a) moving common objects in daily life, such as balls and wooden blocks;

b) picking up a fork and eating a piece of cake with the fork;

c) picking up a spoon and adding sugar to a cup with the spoon;

d) unscrewing a bottle cap and drinking water in the bottle;

e) pinching and drawing a card from a pack;

f) picking up a key to open a lock;

g) threading a needle;

Figure 11, the Supplementary Video shows the experimental results. These results exhibit that both patients can accomplish all tasks with the assistance of the foot-controlled hand/forearm exoskeleton. For bimanual operation tasks, the patient's limb on the unaffected side can coordinate with the paretic limb assisted by the exoskeleton. These experimental results demonstrate that the foot-controlled hand/forearm exoskeleton can restore many voluntary ADLs in patients with chronic hemiparetic upper limbs.

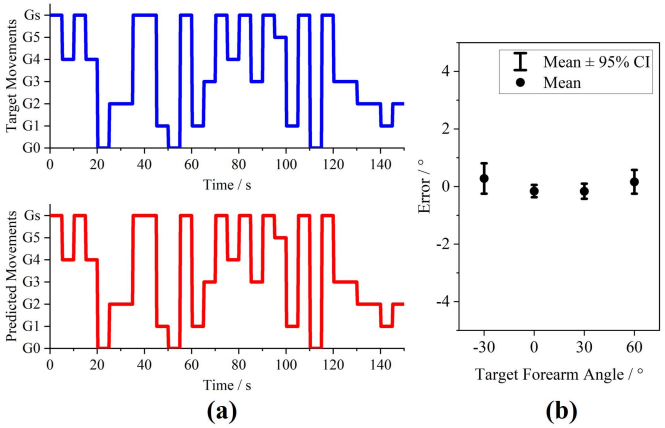

Fig. 10. Evaluation of the FMI. (a) During hand control, the patient is can easily switch hand gesture and perform every gesture with success rate of 100%. G_S is the foot gesture G_{switch}. (b) During forearm control, the patient can rotate his forearm with a static error of less than 1.7°.

D. Discussions

This study presents a foot-controlled hand/forearm exoskeleton that enables patients with chronic hemiparesis to restore their voluntary bimanual ADLs. The exoskeleton can simultaneously provide both active hand gestures and forearm rotation assistances. In this study, we demonstrate the stroke patient 1 is able to accomplish all real-life tasks with the assistance of the foot-controlled hand/forearm exoskeleton. The stroke patient 2 can also accomplish all tasks with the assistance of the foot-controlled hand/forearm exoskeleton except task d. Since his shoulder and elbow are weak, he has to pour the water into a cup instead of directly drinking from the bottle as shown in the Supplementary Video. Therefore, the exoskeleton is suitable for patients with full or partial shoulder and elbow mobility but without hand and forearm mobility. Additionally, the FMI provides patients with an easy and intuitive operation of six hand gestures and continuous forearm P/S control. Compared to existing studies about foot control, proposed FMI has following advantages: 1) As opposed to IMU-based FMIs, the proposed FMI is easy to use because no complicated re-zero procedures are necessary. 2) In contrast to devices controlled using EMG of legs, misclassification of hand/forearm movements caused by biomechanical coupling between leg movements does not occur in the proposed exoskeletons. Therefore, the patient can control six hand gestures with a success rate of 100%. 3) On the basis of FMIs using each pressure sensor separately, a combination of sensor outputs is used to increase the number of user control inputs to operate large degree-of-freedom movements of the hand/forearm exoskeleton. The proposed FMI can control up to 16 hand gestures, which has been discussed in Section II-C. The method is suitable

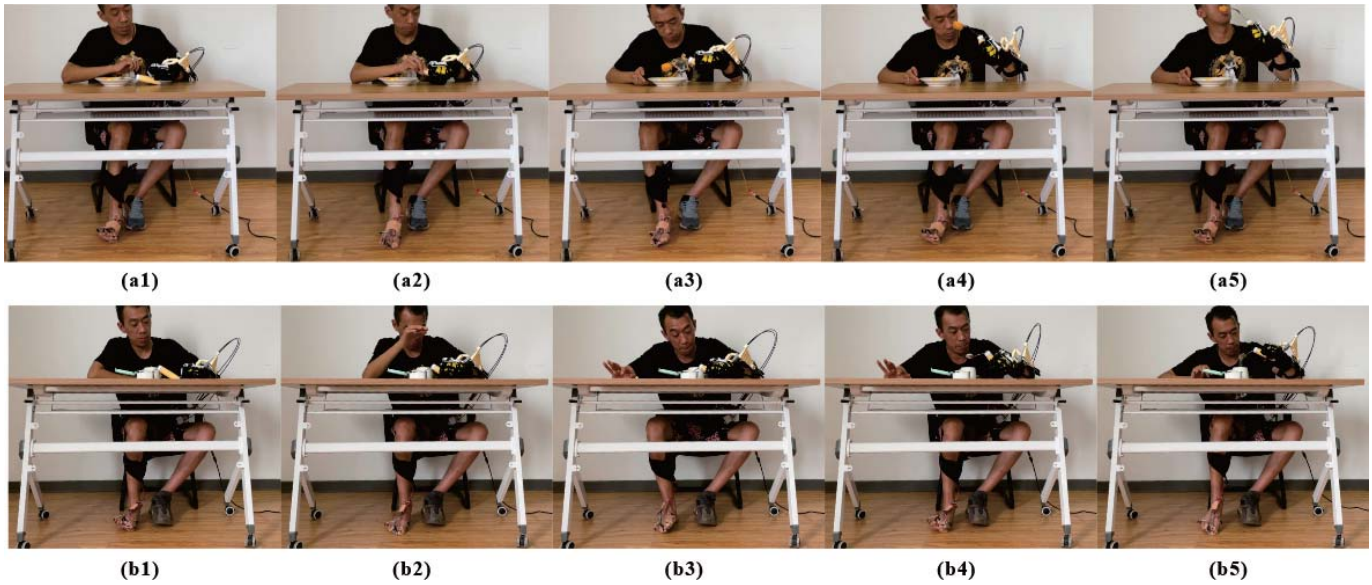

Fig. 11. Examples of ADLs performed voluntarily by the stroke patient 1 with the assistance of the foot-contolled hand/forearm exoskeleton. The 1st example (Picking up a fork and eating a piece of cake using the fork) can be broken down into the following steps: (a1) starting; (a2) grasping the fork; (a3) control mode switch; (a4) forearm supination; (a5) eating. The 2nd example (Picking up a spoon and adding sugar to a cup using the spoon) can be broken down into the following steps: (b1) starting; (b2) grasping the spoon; (b3) control mode switch; (b4) forearm supination and loading the spoon with sugar; (b5) forearm pronation and adding sugar to a cup. The patient gave his permission for this photograph to be reproduced.

for most stroke patients because their unaffected foot can be used to operate FMI. Furthermore, patients with upper limb amputation may benefit from the foot-controlled prosthetic arm.

Also, cognitive impairment may be a factor limiting the applicability of the foot-control hand/forearm exoskeleton. In this study, the cognitive level of the stroke patient 2 is significantly weaker than that of the stroke patient 1, especially in language expression and comprehension. In the experiment, the stroke patient 2 is required to spend more training time than stroke patient 1 to be familiar with the foot gestures and their mapping to hand gestures. However, the stroke patient 2 can also voluntarily operate the foot-controlled hand/forearm exoskeleton to accomplish real-life tasks. It is indicated that cognitive impairment doesn't affect the hand-foot coordination of stroke patients, which will be further confirmed by increasing the number of stroke participants in our future study. In addition, long-term training is believed to improve the dexterity of the patient's foot to accurately control larger number of hand gestures and arm movements.

However, this experimental study had several limitations. First, we observed that the forearm P/S range of the patient was reduced when the spastic muscle tone increased, indicating that the forearm assistance mechanism can be further improved to deal with the large resistance torque of the forearm P/S. Second, plantar pressure can be utilized to control the grasping force of the hand exoskeleton, which will be explored in our future study to improve the grasping quality of patients in their ADLs. Finally, the proposed FMI is applied barefoot in this study to avoid reduced accuracy caused by different sensor locations every time patients wear shoes or socks. We will integrate more plantar sensors into insoles or shoes in our future study to make the FMI easier to use.

V. Conclusion

This study proposes a foot-controlled hand/forearm exoskeleton to allow chronic hemiparetic patients to restore their voluntary bimanual activities. Moreover, we evaluated the effectiveness of the foot-controlled hand/forearm exoskeleton for daily life assistance in two chronic hemiparetic patients. The experimental results presented in Section IV indicate that one of the patients can perform six hand gestures with success rates of 100% and 107° forearm P/S movements, with a static control error less than 1.7°. Through the coordination between the unaffected and paretic limbs, assisted by the foot-controlled hand/forearm exoskeleton, both patients can restore many voluntary ADLs, such as unscrewing the bottle cap, drinking, and eating. This study provides a new approach toward restoring the activities of patients with hemiparesis.

References

[1] V. L. Feigin et al., "World stroke organization (WSO): Global stroke fact sheet 2022," *Int. J. Stroke.*, vol. 17, no. 1, pp. 18–29, 2022.
[2] S. M. Hatem et al., "Rehabilitation of motor function after stroke: A multiple systematic review focused on techniques to stimulate upper extremity recovery," *Frontiers Hum. Neurosci.*, vol. 10, p. 442, Sep. 2016.
[3] K. D. Capek, B. D. Hughes, and G. D. Warden, "Functional sequelae and disability assessment," in *Total Burn Care*. Amsterdam, The Netherlands: Elsevier, 2018, pp. 673–678.
[4] D. H. Kim, Y. Lee, and H.-S. Park, "Bioinspired high-degrees of freedom soft robotic glove for restoring versatile and comfortable manipulation," *Soft Robot.*, vol. 9, no. 4, pp. 734–744, Aug. 2021.
[5] P. Tran et al., "FLEXotendon glove-III: Voice-controlled soft robotic hand exoskeleton with novel fabrication method and admittance grasping control," *IEEE/ASME Trans. Mechatronics*, vol. 27, no. 5, pp. 3920–3931, Oct. 2022.
[6] N. Singh, M. Saini, S. Anand, N. Kumar, M. V. P. Srivastava, and A. Mehndiratta, "Robotic exoskeleton for wrist and fingers joint in post-stroke neuro-rehabilitation for low-resource settings," *IEEE Trans. Neural Syst. Rehabil. Eng.*, vol. 27, no. 12, pp. 2369–2377, Dec. 2019.
[7] D. Buongiorno, E. Sotgiu, D. Leonardis, S. Marcheschi, M. Solazzi, and A. Frisoli, "WRES: A novel 3 DoF wrist exoskeleton with tendon-driven differential transmission for neuro-rehabilitation and teleoperation," *IEEE Robot. Autom. Lett.*, vol. 3, no. 3, pp. 2152–2159, Jul. 2018.

[8] E. Pezent, C. G. Rose, A. D. Deshpande, and M. K. O'Malley, "Design and characterization of the OpenWrist: A robotic wrist exoskeleton for coordinated hand-wrist rehabilitation," in *Proc. Int. Conf. Rehabil. Robot. (ICORR)*, Jul. 2017, pp. 720–725.

[9] K. B. Lee et al., "Six-month functional recovery of stroke patients: A multi-time-point study," *Int. J. Rehabil. Res. Internationale Zeitschrift fur Rehabilitationsforschung. Revue Internationale de Recherches de Readaptation*, vol. 38, no. 2, p. 173, 2015.

[10] B. B. Kang, H. Choi, H. Lee, and K.-J. Cho, "Exo-glove poly II: A polymer-based soft wearable robot for the hand with a tendon-driven actuation system," *Soft Robot.*, vol. 6, no. 2, pp. 214–227, Apr. 2019.

[11] H. K. Yap et al., "A fully fabric-based bidirectional soft robotic glove for assistance and rehabilitation of hand impaired patients," *IEEE Robot. Autom. Lett.*, vol. 2, no. 3, pp. 1383–1390, Jul. 2017.

[12] S. Soekadar et al., "Hybrid EEG/EOG-based brain/neural hand exoskeleton restores fully independent daily living activities after quadriplegia," *Sci. Robot.*, vol. 1, no. 1, Dec. 2016, Art. no. eaag3296.

[13] N. Secciani, A. Topini, A. Ridolfi, E. Meli, and B. Allotta, "A novel point-in-polygon-based sEMG classifier for hand exoskeleton systems," *IEEE Trans. Neural Syst. Rehabil. Eng.*, vol. 28, no. 2, pp. 3158–3166, Dec. 2020.

[14] L. Randazzo, I. Iturrate, S. Perdikis, and J. D. R. Millán, "Mano: A wearable hand exoskeleton for activities of daily living and neurorehabilitation," *IEEE Robot. Autom. Lett.*, vol. 3, no. 1, pp. 500–507, Nov. 2017.

[15] S. Dunaway, D. B. Dezsi, J. Perkins, D. Tran, and J. Naft, "Case report on the use of a custom myoelectric elbow–wrist–hand orthosis for the remediation of upper extremity paresis and loss of function in chronic stroke," *Mil. Med.*, vol. 182, no. 7, pp. e1963–e1968, Jul. 2017.

[16] P. Tran, S. Jeong, S. L. Wolf, and J. P. Desai, "Patient-specific, voice-controlled, robotic FLEXotendon glove-II system for spinal cord injury," *IEEE Robot. Autom. Lett.*, vol. 5, no. 2, pp. 898–905, Apr. 2020.

[17] D. Kim et al., "Eyes are faster than hands: A soft wearable robot learns user intention from the egocentric view," *Sci. Robot.*, vol. 4, no. 26, Jan. 2019, Art. no. eaav2949.

[18] M. B. Hong, S. J. Kim, Y. S. Ihn, G.-C. Jeong, and K. Kim, "KULEX-hand: An underactuated wearable hand for grasping power assistance," *IEEE Trans. Robot.*, vol. 35, no. 2, pp. 420–432, Apr. 2019.

[19] S. Park et al., "User-driven functional movement training with a wearable hand robot after stroke," *IEEE Trans. Neural Syst. Rehabil. Eng.*, vol. 28, no. 10, pp. 2265–2275, Sep. 2020.

[20] S. Hazubski, H. Hoppe, and A. Otte, "Non-contact visual control of personalized hand prostheses/exoskeletons by tracking using augmented reality glasses," *3D Printing Med.*, vol. 6, no. 1, pp. 1–3, Dec. 2020.

[21] Y. Huang et al., "Performance evaluation of a foot interface to operate a robot arm," *IEEE Robot. Autom. Lett.*, vol. 4, no. 4, pp. 3302–3309, 2019.

[22] A. Mirbagheri et al., "Operation and human clinical trials of robolens: An assistant robot for laparoscopic surgery," *Frontiers Biomed. Technol.*, vol. 2, no. 3, pp. 184–190, 2015.

[23] J. M. Sackier and Y. Wang, "Robotically assisted laparoscopic surgery," *Surgical Endoscopy*, vol. 8, no. 1, pp. 63–66, 1994.

[24] S. Voros, G.-P. Haber, J.-F. Menudet, J.-A. Long, and P. Cinquin, "ViKY robotic scope holder: Initial clinical experience and preliminary results using instrument tracking," *IEEE/ASME Trans. Mechatronics*, pp. 879–886, Dec. 2010.

[25] Y. Huang, E. Burdet, L. Cao, P. T. Phan, A. M. H. Tiong, and S. J. Phee, "A subject-specific four-degree-of-freedom foot interface to control a surgical robot," *IEEE/ASME Trans. Mechatronics*, vol. 25, no. 2, pp. 951–963, Apr. 2020.

[26] E. Velloso, J. Alexander, A. Bulling, and H. Gellersen, "Interactions under the desk: A characterisation of foot movements for input in a seated position," in *Proc. IFIP Conf. Hum.-Comput. Interact.* Springer, 2015, pp. 384–401.

[27] K. R. Lyons and S. S. Joshi, "Upper limb prosthesis control for high-level amputees via myoelectric recognition of leg gestures," *IEEE Trans. Neural Syst. Rehabil. Eng.*, vol. 26, no. 5, pp. 1056–1066, May 2018.

[28] L. Resnik, S. L. Klinger, K. Etter, and C. Fantini, "Controlling a multi-degree of freedom upper limb prosthesis using foot controls: User experience," *Disab. Rehabil., Assist. Technol.*, vol. 9, no. 4, pp. 318–329, 2014.

[29] P. Kieliba, D. Clode, R. O. Maimon-Mor, and T. R. Makin, "Robotic hand augmentation drives changes in neural body representation," *Sci. Robot.*, vol. 6, no. 54, p. eabd7935, May 2021.

[30] M. C. Carrozza et al., "A wearable biomechatronic interface for controlling robots with voluntary foot movements," *IEEE/ASME Trans. Mechatronics*, vol. 12, no. 1, pp. 1–11, Feb. 2007.

[31] W. Chen et al., "Soft exoskeleton with fully actuated thumb movements for grasping assistance," *IEEE Trans. Robot.*, vol. 38, no. 4, pp. 2194–2207, Aug. 2022.

[32] A. Kapandji, "Biomechanics of pronation and supination of the forearm," *Hand clinics*, vol. 17, no. 1, pp. 22–111, 2001.

[33] J. Chen and P. S. Lum, "Pilot testing of the spring operated wearable enhancer for arm rehabilitation (SpringWear)," *J. Neuroeng. Rehabil.*, vol. 15, no. 1, pp. 1–11, Dec. 2018.

[34] K.-Y. Wu, Y.-Y. Su, Y.-L. Yu, C.-H. Lin, and C.-C. Lan, "A 5-degrees-of-freedom lightweight elbow-wrist exoskeleton for forearm fine-motion rehabilitation," *IEEE/ASME Trans. Mechatronics*, vol. 24, no. 6, pp. 2684–2695, Dec. 2019.

[35] S.-H. Park, J. Yi, D. Kim, Y. Lee, H. S. Koo, and Y.-L. Park, "A lightweight, soft wearable sleeve for rehabilitation of forearm pronation and supination," in *Proc. 2nd IEEE Int. Conf. Soft Robot. (RoboSoft)*, Apr. 2019, pp. 636–641.

[36] J. Realmuto and T. Sanger, "A robotic forearm orthosis using soft fabric-based helical actuators," in *Proc. 2nd IEEE Int. Conf. Soft Robot. (RoboSoft)*, Apr. 2019, pp. 591–596.

[37] S. W. Lee, K. A. Landers, and H.-S. Park, "Development of a biomimetic hand exotendon device (BiomHED) for restoration of functional hand movement post-stroke," *IEEE Trans. Neural Syst. Rehabil. Eng.*, vol. 22, no. 4, pp. 886–898, Jul. 2014.

[38] T. Tsuji, N. Bu, O. Fukuda, and M. Kaneko, "A recurrent log-linearized Gaussian mixture network," *IEEE Trans. Neural Netw.*, vol. 14, no. 2, pp. 304–316, Mar. 2003.

[39] T. Flash and N. Hogan, "The coordination of arm movements: An experimentally confirmed mathematical model," *J. Neurosci.*, vol. 5, no. 7, pp. 1688–1703, Jul. 1985.

[40] C. Wang, L. Peng, and Z.-G. Hou, "A control framework for adaptation of training task and robotic assistance for promoting motor learning with an upper limb rehabilitation robot," *IEEE Trans. Syst., Man, Cybern. Syst.*, vol. 52, no. 12, pp. 7737–7747, Dec. 2022.

[41] E. Ayhan and C. C. Ayhan, "Kinesiology of the elbow complex," in *Comparative Kinesiology of the Human Body*. Amsterdam, The Netherlands: Elsevier, 2020, pp. 191–210.